

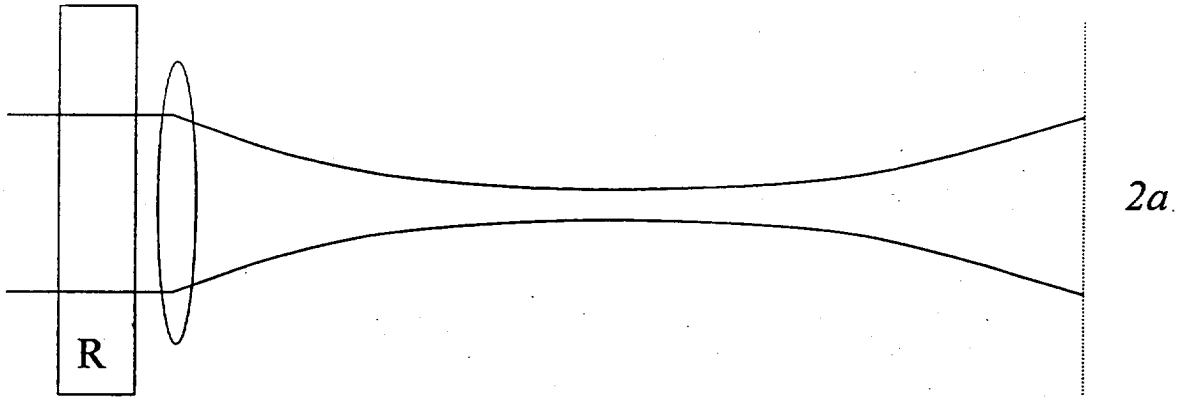
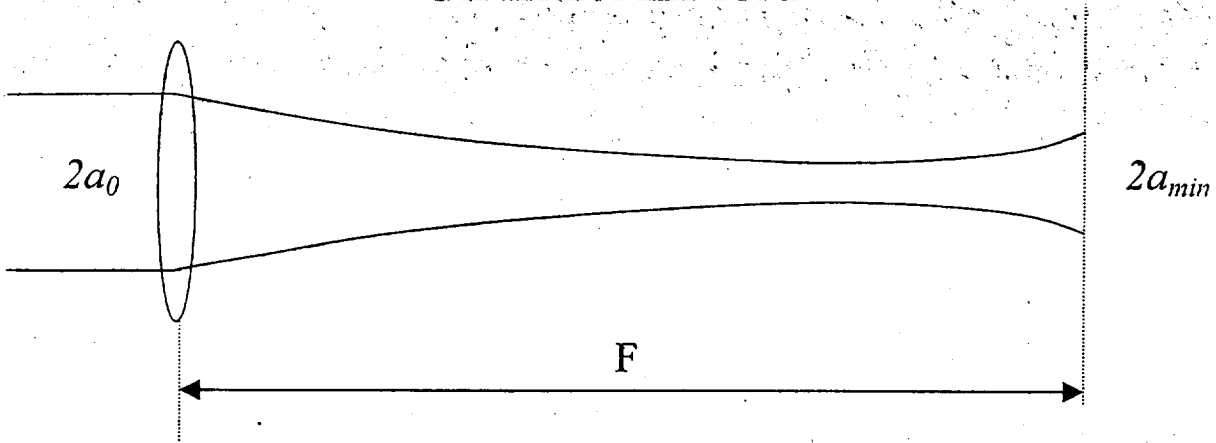
Wavefront Characterization of
Large Optics

N. Andreev, E. Khazanov, I. Kojevator,
A. Mal'shakov, A. Potyomkin, A. Sergeev

IAP, Nizhny Novgorod, Russia

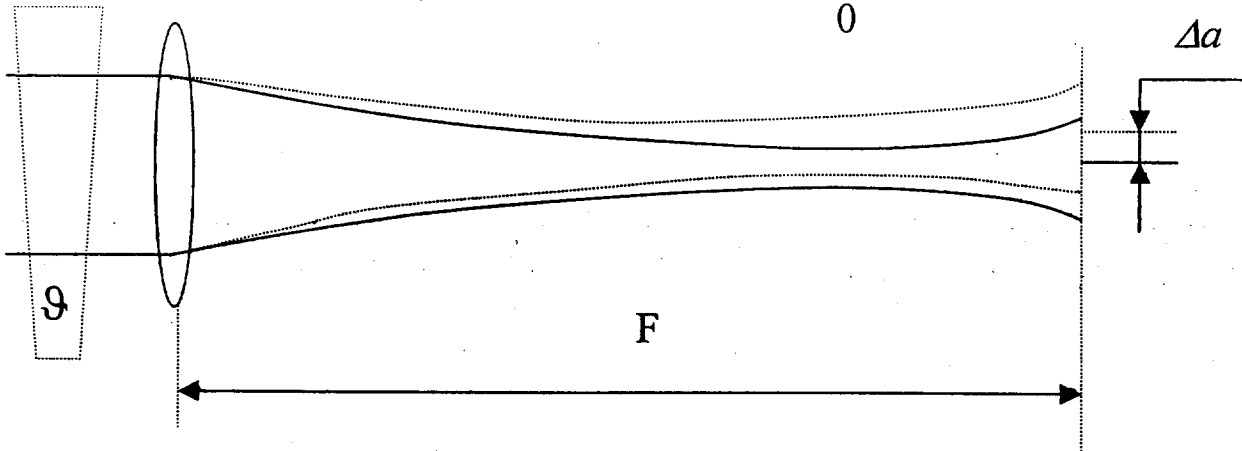
LSC Meeting, Livingston, LA

LINEAR MEDIUM



$$a_{min} = F \vartheta_{min} \quad a = a_{min} \sqrt{1 + (z_d / R)^2} \quad z_d = (2\pi / \lambda) a_0^2$$

$$\text{if } \Delta a = 0.1a \quad |R_{max}| \approx 2.18z_d \quad \Delta z = a_0^2 / 2R = \lambda / 27$$

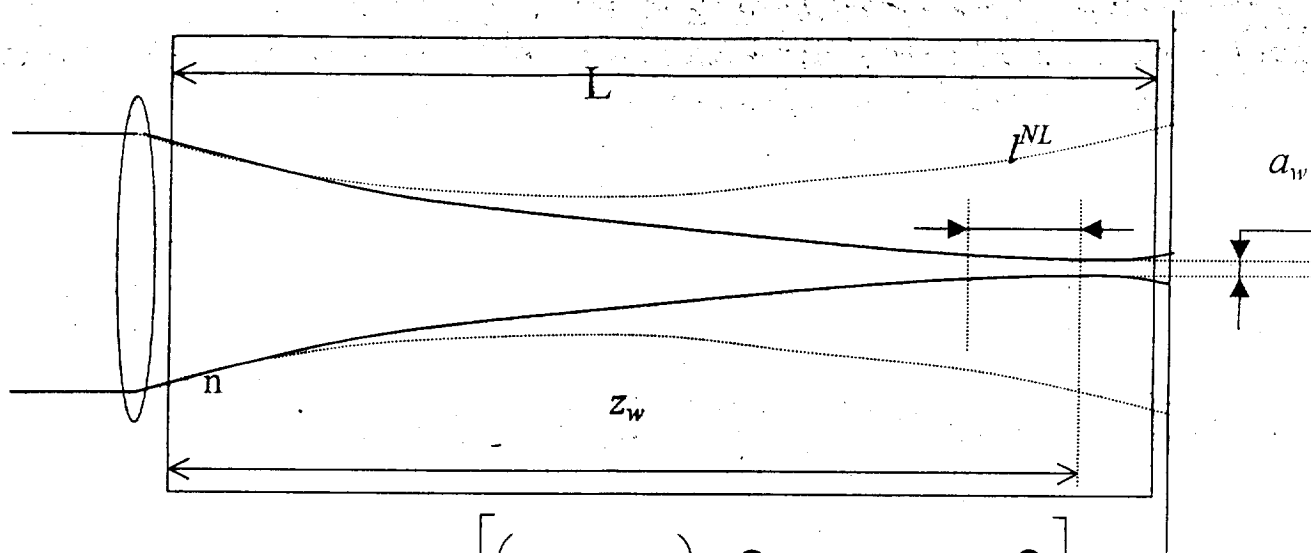


$$\Delta a = gF$$

$$\Delta a = 0.1a$$

$$\Delta z = \lambda / 20\pi$$

NONLINEAR MEDIUM



$$a^2(z) = a_0^2 \left[\left(1 - \frac{P}{P_{cr}} \right) \frac{z^2}{z_d^2} + \left(1 - \frac{z}{nF} \right)^2 \right]$$

$$z_w = \frac{nF}{1 + \left(\frac{F}{z_d} \right)^2 \left(1 - \frac{P}{P_{cr}} \right)}$$

$$a_w^2 = a_0^2 \left(1 - \frac{z_w}{Fn} \right)$$

$$l^{NL} = \frac{z_d n}{1 - \frac{P}{P_{cr}}} \left(1 - \left[1 + \left(\frac{F}{z_d} \right)^2 \left(1 - \frac{P}{P_{cr}} \right) \right]^{-1} \right)$$

Advantage of the nonlinear methods.

$$\frac{a^2}{a_{\min}^2} \sqrt{1 - \frac{P}{P_{cr}}}$$

$$a/a_{\min}$$

EXPERIMENTAL SETUP AND TECHNIQUE

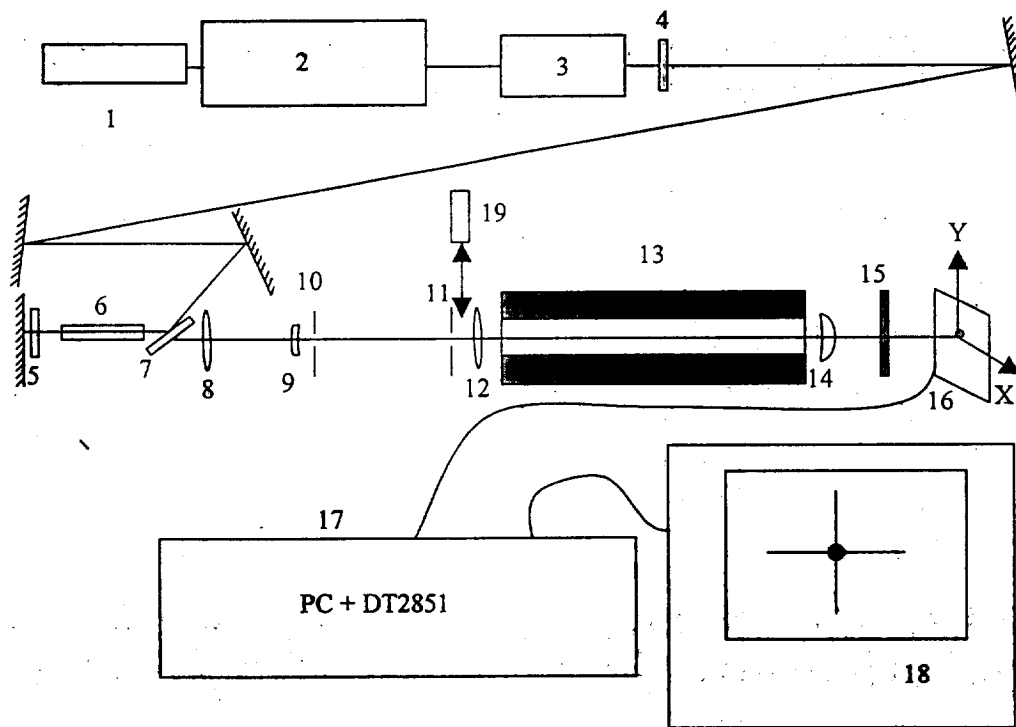


Fig.1. Schematic optical diagram of the experimental setup
 1- HeNe laser, 2-Nd glass master oscillator, 3-Single pulse selector, 4- $\lambda/2$, 5- $\lambda/4$, 6-Nd Glass amplifier, 7-Polarizer, 8-Lens $F_1=+33.5$ cm, 9-Lens $F_2=-7.5$ cm, 10-pinhole $\varnothing 0.6$ mm, 11-pinhole $\varnothing 0.8$ mm, 12- $F_3=+28$ cm, 13-Bensen cell ($L=40$ cm), 14-Lens $F_4=+4.5$ cm, 15-Attenuator, 16-CCD camera, 17-PC+Frame Grabber DT2851, 18-Analog monitor, 19-Sample.

CHOICE OF A NONLINEAR MEDIUM

TABLE I
Transverse size of self-focusing points

Substance	Radius of «self-focusing» point» at e^{-1}	Pulse duration	Length of nonlinear cell
Phosphate laser glass ^a	40 μm	170 psec	60 cm
Toluene ^a	90 μm	170 psec	60 cm
Benzene ^a	5 μm	170 psec	60÷30 cm
Methylene chloride ^a	23 μm	170 psec	60 cm
Silicate laser glass ^b	25 μm	1-2 nsec	72 cm
Water ^c	15-30 μm	1-2 nsec	66 cm
Nitrobenzene ^d	3.6 μm	Several psec.	Several cm
Toluene ^e	10 μm	Several psec.	Several cm

^a Data of the present work

^b A.N.Malshakov, G.A.Pasmanik, and A.K.Potyomkin, "Comparative characteristics of magneto-optical materials", *Applied Optics*, **36**(8), pp.6403-6410, 1997.

^c A.I. Makarov, A.N. Mal'shakov, and A.K. Potemkin, "Measurement of small distortions of the wavefront of laser radiation," *Optics and Spectroscopy*, **86**(1), pp.134-137, 1999.

^d S.L.Shapiro, *Ultrashort Light Pulses*, Springer-Verlag Berlin Heidelberg New York, p.163, 1977.

^e Y. R. Shen, *Self-focusing: Experimental*, Progress in Quantum Electronics, **4**(Part I), p. 3, 1975.

RESULTS AND DISCUSSION

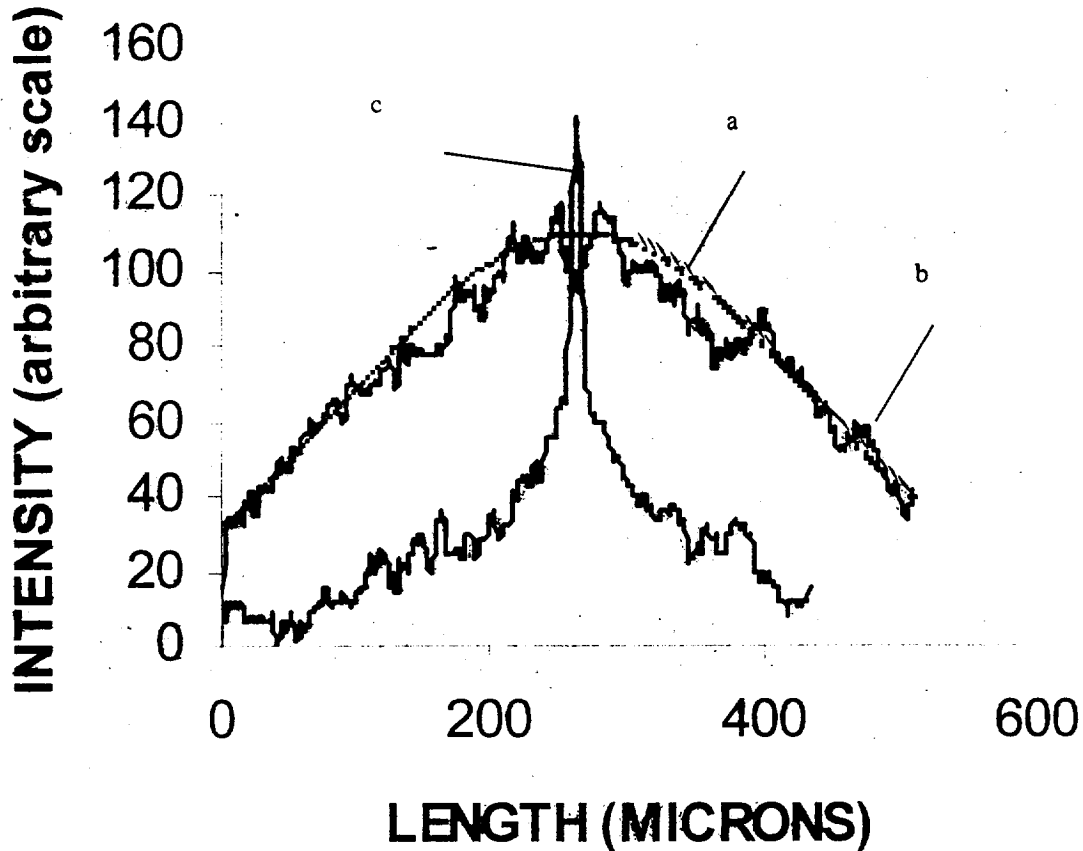


Fig.2. Cross section of laser radiation intensity at the output window of the cell filled with benzene. Curve **b** is the linear case, i.e., when power in a pulse is much less than the threshold self-focusing power $P \ll P_{thr}$. Curve **c** is when $P_{thr} < P < 2P_{thr}$ at beam self-focusing. Curve **a** is a gaussian fit of curve **b** $I(r) = I_0 \exp(-(r/a)^2)$ where $a = 280 \mu\text{m}$. The sizes of the CCD camera were too small to resolve the self-focusing point at one magnification and to see the whole diffraction spot in the absence of the self-focusing.

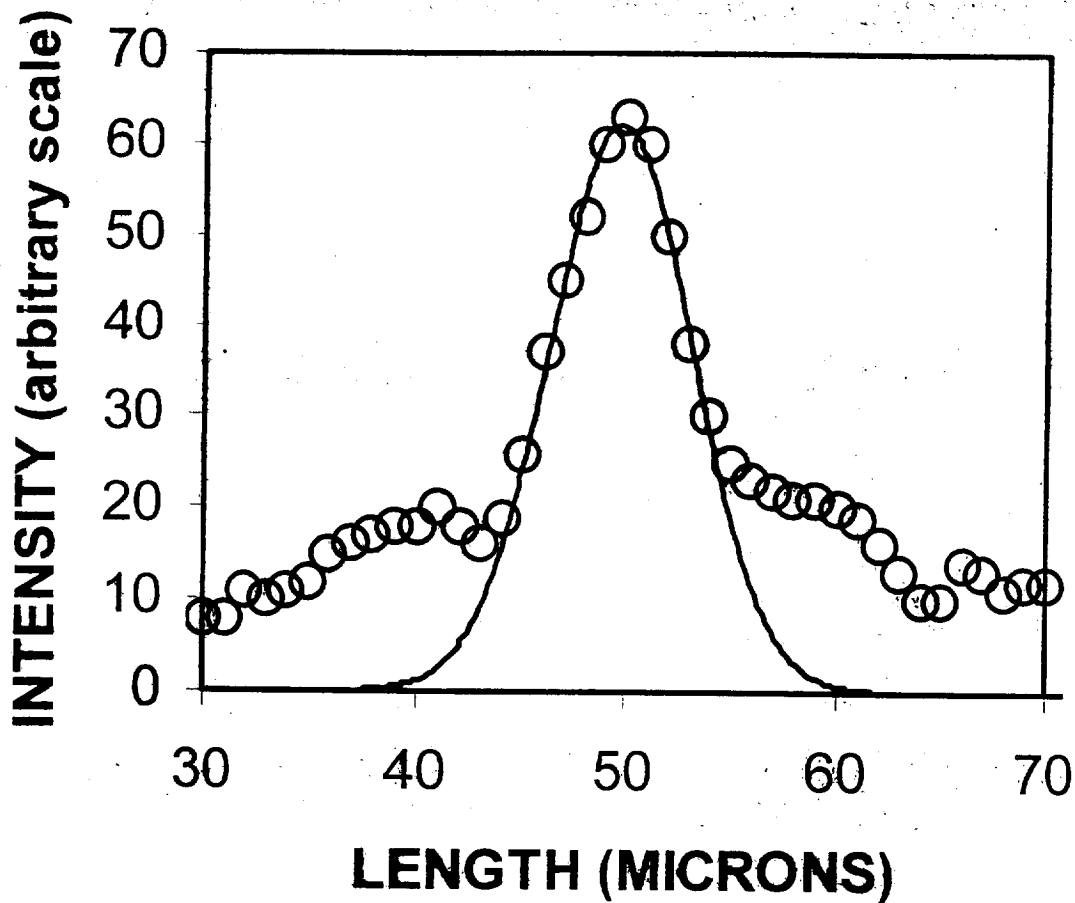


Fig.3. Fragment of the cross section of the self-focusing point. Circles indicate experimental data obtained by computer processing of a CCD camera frame; solid curve is gaussian fit $I(r) = I_0 \exp(-(r/a_{min})^2)$ where $a_{min} = 5 \mu\text{m}$.

$$N < 100.$$

$$Stdev(x) \approx 3.5 \mu\text{rad} \text{ and } Stdev(y) \approx 4.8 \mu\text{rad}.$$

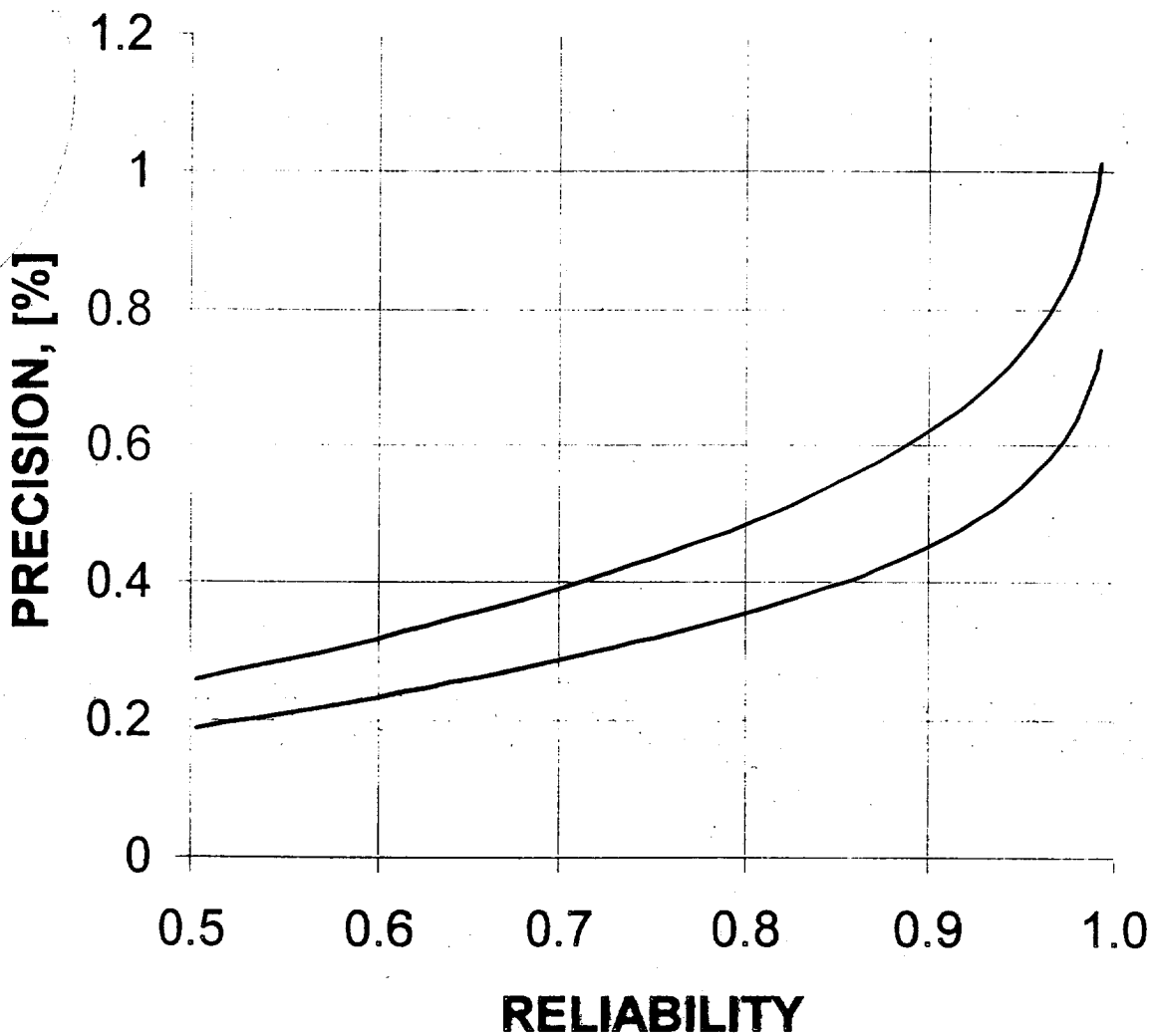
$$g_{\text{dif}} = 500 \mu\text{rad}$$

$$\Phi(a) = \frac{2}{\pi} \frac{1}{\sigma} \int_0^a \exp\left(-\frac{x^2}{2\sigma^2}\right) dx.$$

For a median error as a criterion of an error $\Phi(\Delta g/g_d) = 0.5$,

$$\Delta g/g_d < 0.2-0.3 \%$$

$$\Delta z = \Delta g \cdot a, \quad \Delta z = \lambda/M = \lambda/3000$$



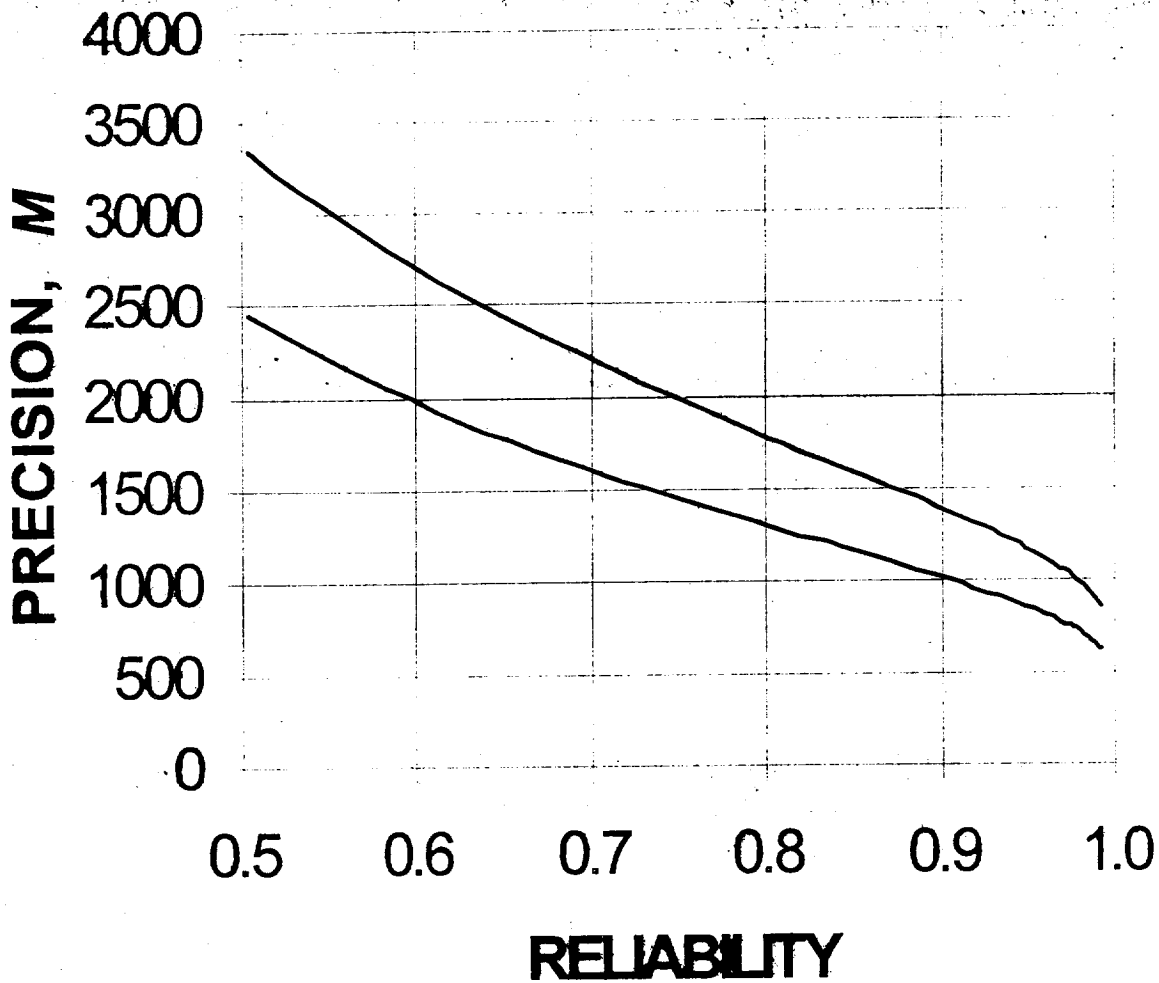


Fig.5. Accuracy of determination of the wavefront distortions $\Delta z = \lambda/M$ in terms of wavelengths as a function of the reliability $\Phi(\Delta z)$. The top curve is for horizontal direction, the bottom curve is for vertical direction.

PHASE-MODULATED WHITE-LIGHT INTERFEROMETER

1. The possibility of tuning the illuminated light spectrum according to the distance between the measured and reference surfaces to suppress interference with other reflections. This may be important in the case of non-uniform cross-section reflectance distributions.
2. The possibility to avoid the influence of secondary reflections on interference patterns.
3. The absence of any speckle-inhomogeneity in the interference pattern. Speckle plagues coherent laser illumination.
4. There is no modulation of distance between the interferometric surfaces. Thus, the sample and reference plates are quiet during measurements. This is a *significant* advantage over conventional phase interferometers for characterizing massive, wide-aperture optics.

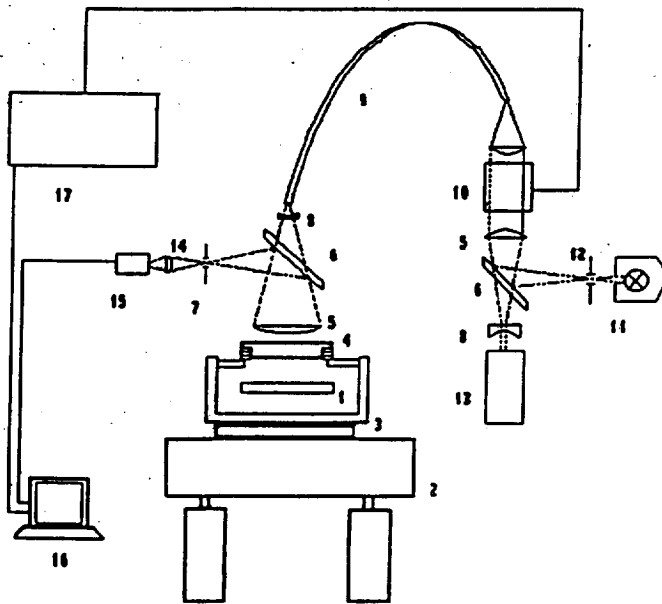


Fig.1. Scheme of interferometer.

Here: 1 - sample; 2 - stabilized optical table; 3 - damping mount; 4 - reference plate; 5 - collimating lens; 6 - beam-splitters; 7 - spatial filter; 8 - lens; 9 - fiber bundle; 10 - illuminating light spectral modulator; 11 - white light source; 12 - aperture; 13 - frequency stabilized He-Ne laser; 14 - projection lens; 15 - CCD-camera; 16 - computer; 17 - synchronization and control block

HIGH-PRECISION ($\lambda/1000$) CHARACTERIZATION OF OPTICAL SURFACE QUALITY USING PHASE-MODULATED WHITE-LIGHT INTERFEROMETER

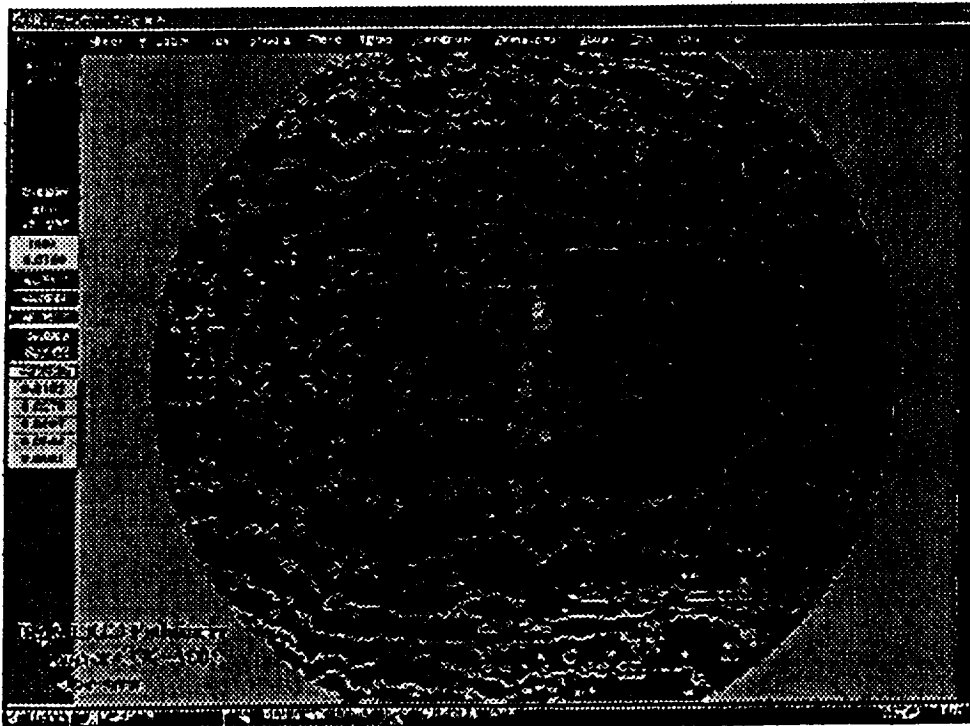
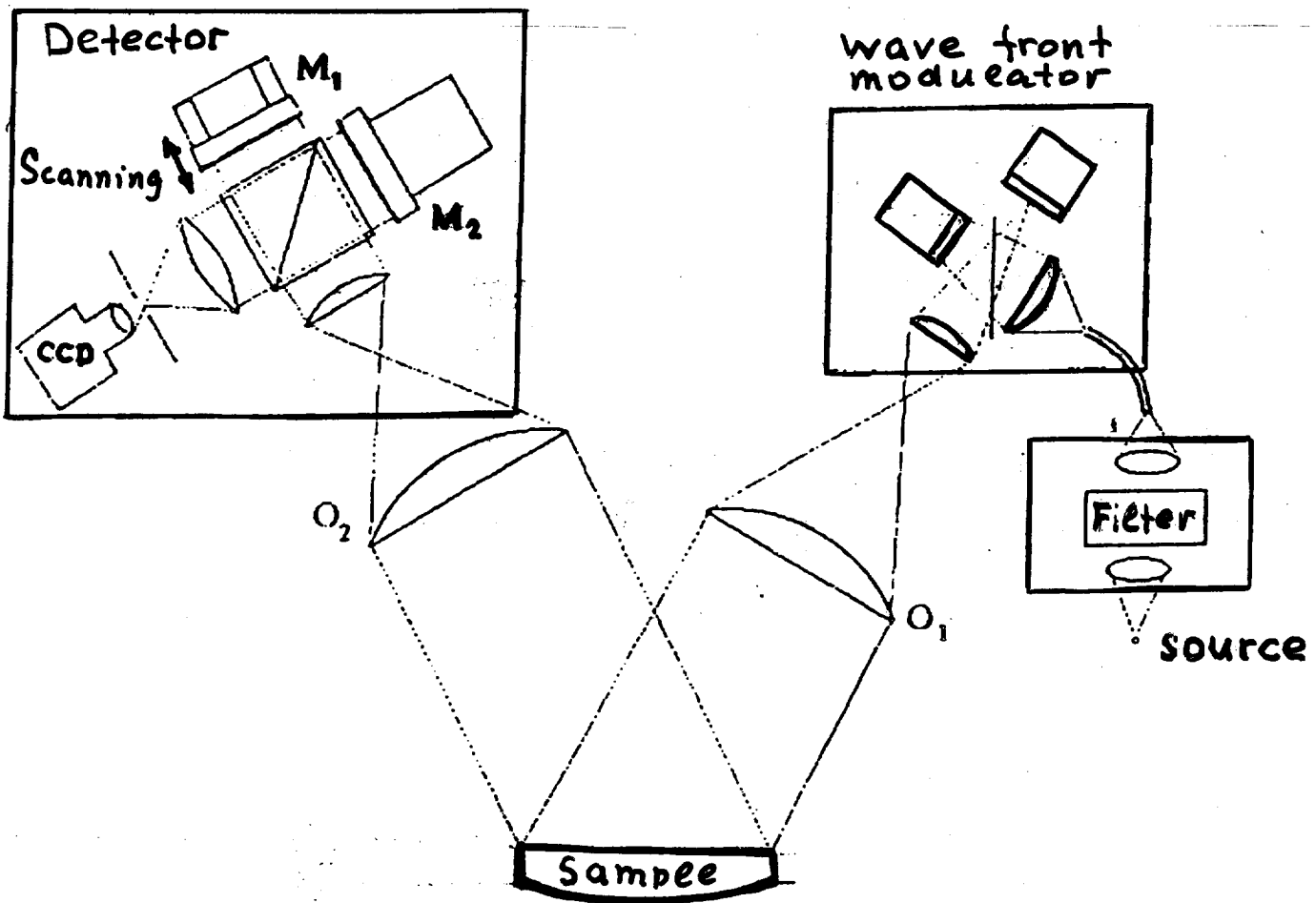


Figure 2 - Phase Map
of the LIGO
Pathfinder Optic
COC-A005

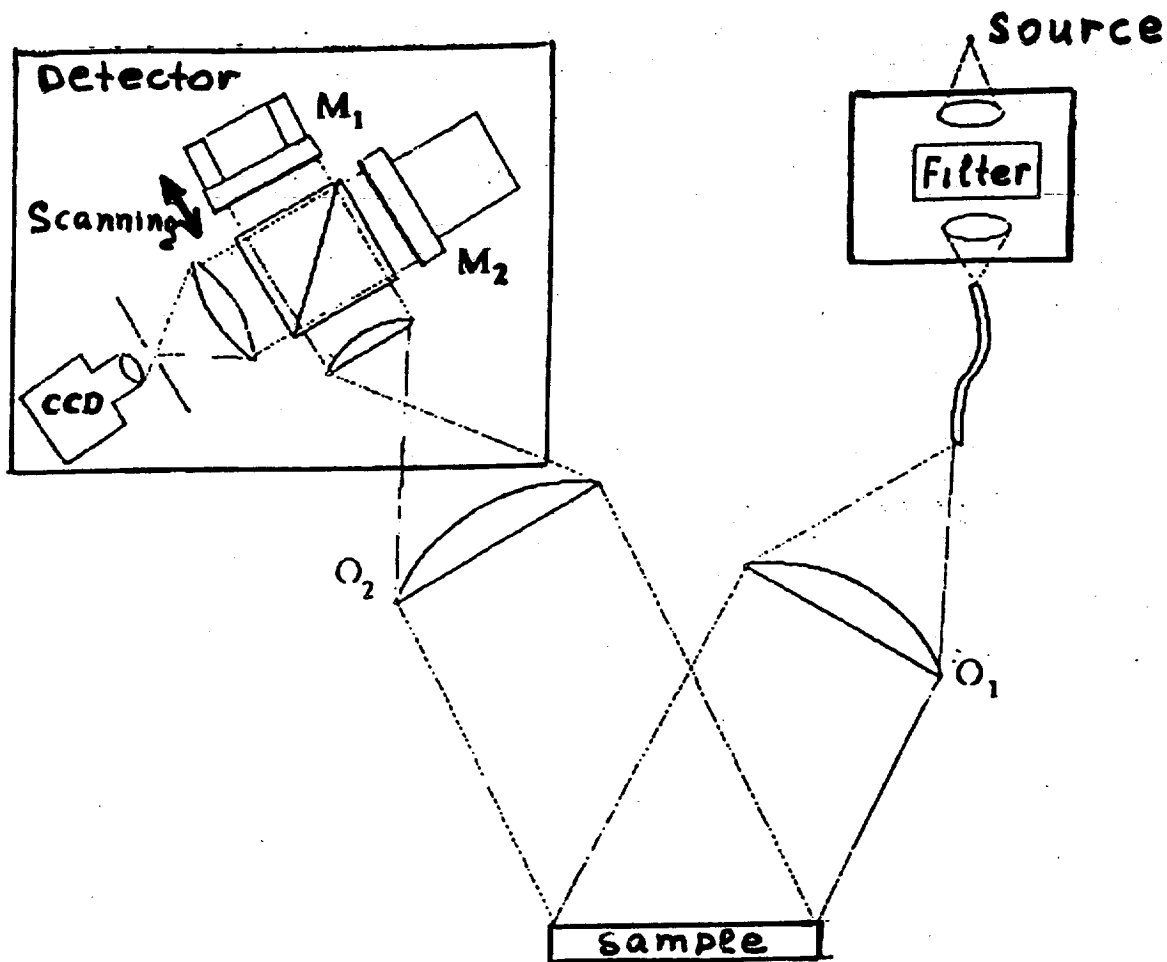
The setup has demonstrated the following characteristics:

- root-mean-square accuracy $\lambda/1000$;
- scale of the irregularities (in the processing area) from several microns to 80 mm;
- processing area 60 x 80 mm;
- measuring and processing time for a 240 x 320 pixel phase pattern less than 10 min.

SCHEMATIC OF PHASE-MODULATED "WHITE-LIGHT" INTERFEROMETER FOR IN SITU MAPPING OF OPTICAL THICKNESS (spherical components)



SCHEMATIC OF PHASE-MODULATED "WHITE-LIGHT" INTERFEROMETER FOR *IN SITU* MAPPING OF OPTICAL THICKNESS



Note 1, Linda Turner, 05/17/00 10:33:03 AM
LIGO-G000145-00-D